京都大学防災研究所年報 第 54 号 B 平成 23 年 6 月
Annuals of Disas. Prev. Res. Inst., Kyoto Univ., No. 54 B, 2011

A Study on Mechanism of the Limestone Debris Flow and its Flow Characteristics

Mohd Remy Rozainy M. A. Z*, Yosuke YAMASHIKI, Taku MATSUMOTO, Tamotsu TAKAHASHI and Kaoru TAKARA

* Graduate School of Engineering, Kyoto University

Synopsis

The steep-slope debris flow experimental channel was employed. It is important to investigate the characteristics of larger particles movement in debris flow as it can cause major damages and casualties. This research demonstrates the debris flow development mechanism between two different particle sizes. Two different sizes of particles were 10mm and 2.5mm. This study involves one slope angle which is 25º. A constant discharge (3.0l/s) was supplied for the duration of 7 seconds. The particle movement was visually analyzed by using high speed video camera (HSVC) to capture the movement characteristics of the individual particle grain. A numerical model entitled as the Hydro-Debris 2D Model (HD2DM) was developed based on the Lagrangian sediment particle tracing numerical experiment. The HSVC results tracing each particle movement were compared with the HD2DM simulations. Analyses using the HSVC fully demonstrated the mechanism of the debris flow. Velocities in upper layers are faster than in lower layers and the larger particles move ahead. Similar characteristics can be observed in the numerical simulation using HD2DM.

Keywords: debris flow, high speed video camera (HSVC), lagrangian, hydro-debris 2d model (HD2DM)

1. Introduction

In the recent decade, several debris flow events occurred and caused hundreds of deaths, missing or injury and damaged many facilities. To prevent and mitigate disaster effectively, it is necessary to understand the initiation mechanism of debris flow. In previous study, there seems scare to define the debris flow initiation from engineering mechanism point of view. It is necessary to discuss further into causes, dominant factors and mechanism of debris flow.

Many researchers have their ways to give the definition of the debris flow. Even though the definitions may not the same from one researcher to others and it completely depend on the various characteristics. Debris flows are flows of mixture of soil, rocks and water. These flows are commonly initiated by landslides, bank failure or hills lope failures related to high rainfall and/or large runoff (Jan, 1997). Debris flows include many events such as debris slides, debris torrents, debris floods, mudflows, mudslides, mudspates, hyperconcentrated flow and lahar (Johnson, 1984). Interaction of solid and fluid forces not only distinguishes debris flow physically but also gives them unique destructive power. Because of their high velocities in the order of several meters

per second, they are the most dangerous type of mass movements and cause significant economic loses as well as casualties (Martinez et al., 1995). Debris flow mainly dealt with laboratory simulations (Bagnold, 1954; Van Steijn and Coutard, 1989), modeling trigger and movement mechanisms (Takahashi, 1981 and Takahashi et al., 1992), deposits (Innes, 1985; Strunk, 1991) and case studies of extreme events that caused damage or casualties (Villi and Dal Pra, 2002; Lin and Jeng, 2000). Previous studies have also used video analysis to investigate debris flows (Adam et al., 2008; Inaba et al., 1997; Arattano and Grattoni, 2000; Ikeda and Hara, 2003; Inaba and Itakura 2003; Lavigne et al., 2003; Tecca et al., 2003; Zhang and Chen, 2003).

The assessment of the debris flow hazard potential has to rely on semi-quantitative methods. Due to the complicity of the debris flow process, numerical simulation models of debris flow are still limited with regard to practical applications. This paper starts with the presentation of the description of the model which includes material used, data collections and numerical simulation (HD2DM). This study employs the preliminary numerical method as known as HD2DM to simulate the debris routing mechanism. Comparison results of the experimental model and HD2DM will be discussed and finally conclusions of the particle grains deposition pattern had been made.

2. Description of the model

In order to understand the characteristics of debris flow routing mechanism and the deposition behavior, it is necessary to set up a debris flow experimental physical model. Experimental setup of the debris flow physical model was carried out at the Ujigawa Open Laboratory, Kyoto University. This laboratory provided complete facilities to operate our study in good condition.

The model consists of three main parts which are rectangular flume, deposition board and water intake tank. Details of each component will be discussed in next section. Fig.1 shows the debris flow experimental model.

3. Experimental procedure

Three cases of laboratory experiments are conducted in these studies which are 15°, 20° and 25° slope angles. Experiments were conducted separately but the water discharge was set as same for each case. In this paper, authors only discussed about one slope case which is 25°. To make sure the results were consistent; materials between small and big particles were well mixed up by using special equipments. For each case, at least three time of experiment had been made to understand the limestone particle distribution and movements.

Fig. 1 The debris flow experimental model

After a flume and board were set to the prescribed slopes, a constant discharge was supplied from the upstream end of the channel through an electromagnetic valve (gate). A constant discharge (3.0l/s) is supplied within 7s. During water supply, high speed video camera (HSVC) will recorded the image of particle routing. The HSVC has been placed under the rectangular flume to capture the movement characteristic of the individual particle grain. The HSVC can capture a video footage during short intervals time (0-9s).

Moreover, two video cameras were set at different locations to record continuous and simultaneous of debris flow deposition process. Video had been recorded during experiments. This important procedure should be made for further understanding. Video will be referred during post analysis. The formation of debris flow deposition process can be more understandable by repeating looked at the debris flow movement characteristics.

3.1 Materials

Two different sizes of materials are used. Each material can be easily differentiated by looked at the size. The materials mean sizes were 10mm and 2.5mm respectively. The materials had been used have a same unit weight which are 2.7gcm^{-3}. For single run the total weight of each material is 10kg. Distance of free surface flow appeared 3.5m from the downstream end (deposition board); the part of the bed upstream from this point was unsaturated. The materials lay on the bottom of the channel with a thickness of 10cm. The boundary between small and big materials was assumed to be 0.3mm.

3.2 Flow

To make sure this experiment is conducted with a constant and accurate flow. The author has carried out a flow test by using flow discharge measurement tools. This equipment include two parts which are electrostatic level gauge (model: CWT-100) and it is connected to data logger (model: GL200A). The electrostatic level gauge contain actuator rod which is highly stable water level meter and it is located in the water storage tank.

The discharge data have been collected by data logger will be analyzed by using personal computer. The concept behind this equipment is to calculate a water level between two points. Water heights were obtain before and after water had been supplied during experiment. Fig.2 shows the schematic diagram of the discharge measurement tools.

In order to obtain the standard of flow discharge used for the experiment, six cases of gate height were choose which are 13mm, 14mm, 15mm, 16mm, 17mm and 18mm. Each case is repeated for three to six time. Fig.3 shows the flow test data. As seen from the result, we can conclude that the equipment was run in a good condition and it gives a consistent result. Therefore flow discharge from this test can be used for my study. For the purpose of debris flow experimental study, 16mm height has been selected. This height will produce 3l/s flow discharge.

Gate control is one of the important things to consider since it influent flow discharge. For that reason, automatic gate controller has been used to obtain an accurate result. The automatic gate controller is combination of two equipments which are electric actuator rod (model: RCP2W-RA6C) and controller (model: PCON-C-56PI-NP-2-O). Power supply (model: PS-241) had connected to the controller and from controller it connected to the personal computer. To get height of the gate as what we want, we have to insert the value via controller.

3.3 HSVC and camera setting

To obtain a very clear and quality image of fast moving particle, a HSVC was used. The model of HSVC is Kato Koken High Speed KIII. The dimension of this camera is 160mm x 104mm x 82mm. The system design for this camera is scaleable and network-compatible with standard and/or notebook PCs. Recording time is up to 9s at full resolution. Longer record times with variable resolution and frame rates. Photographing possibility of high resolution 2,900,000 pixel with maximum of 100,000 scene/photographing speed per second. The

shortest exposure time (shutter speed) is 1 millimicrons/sec. This HSVC was compact design which superior in cost performance and can be used for long haul high-speed photographing in 6 hours consecutively with hard disk built-in. Capture device for this camera is 13.568mm x 13.68mm CMOS (complementary metal-oxide semiconductor). Fig.4 shows the image of HSVC has been used in this study. Four groups of time frame were carried out to understand the particle characteristics mechanism. The groups are (a) initial, no liquid-phase flow (b) starting with liquid-phase flow (c) intermediate, 2s and (d) last, 4s.

(a)

(b)

Fig. 4: The HSVC (a) front view (b) back view

To achieve superior performance for fantastic Full HD video and stills, JVC Everio Model GZ-HM570 is used. Two sets of camcorder with ability of 24Mbps high bit rate recording. The advantages of this model are advanced image stabilizer and it can be zooming until 40 times. It is useful especially during post deposition analysis. We can get clear view and accurate shape and height of the deposition. This camera is very important to observe the changes of particles and depositions shape happen during experimental study. These two cameras are located near the deposition board.

4. Data collection

In this study, the data collection can be separate to three parts which are particles routing movements, observation of the material depositions and sampling of the materials. Fig.5 shows the summarized of the steps taken during data collection.

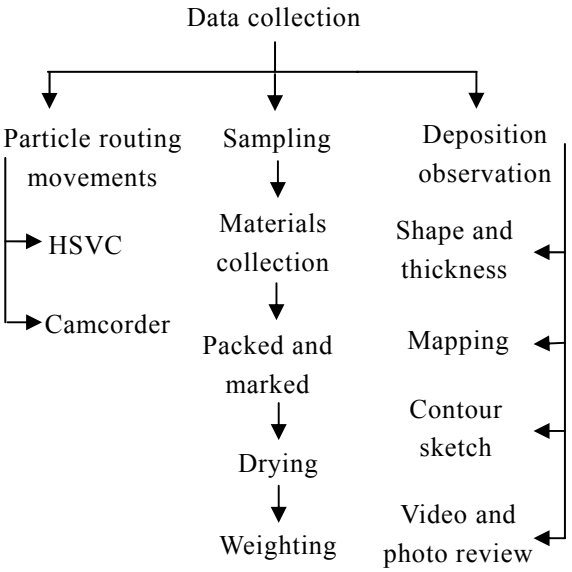

Fig. 5: Steps taken during data collections

4.1 Particle routing movements

In order to investigate the debris flow characteristics routing mechanism, HSVC was used to capture the image. By looking throughout the image movements between big and small particles, the development mechanism of debris flow can be more understand. The images of particle tracing were captured between 0.015s. The distance of particle movements were identified. By knowing the distance of each particle distribution, the velocity of each particle can be calculated.

4.2 Sampling

The objective of the sampling processes is to get the percentage of materials at different node at different height. This process involved four steps. First step was materials collection at certain node that been identified. This method was done by using special equipment made by the author. After that, materials at different height had been packed and marked. Then each packed had to be dried at 105°C for 24 hours. The last step just after drying process was by take a weight of each sample.

4.3 Deposition observation

The objectives of this method are to understand the particle characteristics, particle distribution and the physical data of the deposition materials. Observation of the

deposition processes included (1) measuring deposit shape and thickness distribution, (2) mapping surface structure, (3) deposition contour sketch and (4) reviewing video and still photographs of the stages of the debris deposition formation. These four processes had to be done and repeated more than once time to get the accurate results.

5. HD2DM

The principal aim of a vertical two-dimensional numerical model development is for estimating the particle tracing and mechanism of 10mm and 2.5mm debris. The model development in this study is based on a model developed by Yamashiki et al. (1997). The particle tracing movement can be visually analyzed by using HSVC. A numerical model was developed using the Marker and Cell Method, which involves a SGS (Subgrid-Scale) model and the PSI-Cell (Particle Source in Cell) Method. The transportation processes of debris and air bubble were simulated in Lagrangian form by introducing air bubble and debris markers. Air bubble movement characteristics were simulated by this numerical model.

The systems of governing equations are the grid-filtered time-dependent three-dimensional compressible (with low Mach number) mixed flow Navier-Stokes, liquid phase continuity equations. SGS model for only liquid phase is introduced. The effect of Lagrangian sediment particle into liquid phase is being considered using PSI-CELL method.

Continuity equation for water

$$\frac{\partial}{\partial t} f_L \rho + \frac{\partial}{\partial x_j} f_L \rho \overline{u_j} = 0 \quad (1)$$

$$\frac{D(f_L \rho \overline{u_i})}{Dt} = \frac{\partial}{\partial x_j}(1+f_a+2.5f_S)\mu\left(\frac{\partial \overline{u_i}}{\partial x_j}+\frac{\partial \overline{u_j}}{\partial x_i}-\frac{2}{3}\frac{\partial \overline{u_k}}{\partial x_k}\delta_{ij}\right)$$

$$-\frac{\partial \overline{P}}{\partial x_i}+f_L\rho g_i-\nabla\left\{f_L\rho(R_{ij}+L_{ij}+C_{ij})\right\}+S_{pi} \quad (2)$$

Reynolds term

$$R_{ij}=-2KS_{ij}, S_{ij}=\frac{1}{2}\left(\frac{\partial \overline{u_i}}{\partial x_j}+\frac{\partial \overline{u_j}}{\partial x_i}\right), K=(C_S\Delta)^2\left[2S_{ij}S_{ij}\right]^{1/2} \quad (3)$$

$$\Delta^2 = (\Delta x^2 + \Delta y^2 + \Delta z^2)/3 \quad (4)$$

Leonards term

$$L_{ij}=-\frac{\Delta_k^2\partial^2(\overline{u_i}\overline{u_j})}{24\partial x_k\partial x_k}, C_{ij}=-\frac{\Delta_k^2\overline{u_i}\partial^2(\overline{u_j})}{24\partial x_k\partial x_k}-\frac{\Delta_k^2\overline{u_j}\partial^2(\overline{u_i})}{24\partial x_k\partial x_k} \quad (5)$$

$$S_{pi} = -\frac{\partial \overline{M_{pi}}}{\partial t}, \overline{M_{pi}} = V^{-1}\left(\sum_{k=0}^{k=NS} m_{pk}\, u_{pik}\right) \quad (6)$$

in which f_L, f_g, f_s are volumetric ratio of Liquid (water), gas (air) and solid (sediment) phases, respectively, $i,j,k=1,2,3,$、 u_i velocity component of water in I direction, ρ: water density, p: water pressure, g : gravity force (when i=3) , R_{ij}, C_{ij}, L_{ij} are Reynolds, Cross , Leonards terms, respectively, determined by Kano et al., (1985) Cs : Smagolinsky (1963) coefficient, μ : is water viscosity, $\Delta x, \Delta y, \Delta y$ grid spacing for each direction V: Cell volume, S_{pi} is negative production term for flow field by particle movement, m_{pk} specific mass of particle K, u_{pik} : i direction velocity component of particle k. In which C_D: drag coefficient $\vec{u}_p$ velocity vector of sediment particle (for each diameter), $\vec{u}_f$: water phase velocity vector $\vec{u}_r = \vec{u}_p - \vec{u}_f$ A_2 =p/4 , A_3=p/6 , d : diameter of the sediment C_M: virtual mass coefficient (=0.5), s :density of sediment particle, rho: water density. ε : shading coefficient determined only when sediment is in the bed and shaded by other sediment, μ_f friction coefficient.

Lagrangean sediment transport equation

$$\rho\left(\frac{\sigma}{\rho}+C_M\right)A_3d^3\frac{d\vec{u}_p}{dt}$$

$$=-\frac{1}{2}C_D\rho|\vec{u}_r|\vec{u}_rA_2d^2+\rho(1+C_M)A_3d^3\frac{d\vec{u}_f}{dt}$$

$$+\rho\left(\frac{\sigma}{\rho}-1\right)A_3d^3(g_i-\mu_fg_j) \quad (7)$$

$$C_D = 0.4 + \frac{24}{R_e}; R_e = \frac{|u - u_p|d}{v} \quad (8)$$

Lagrangian air bubble transport equation

$$\rho\beta A_3 a^3 \frac{d\vec{u}_a}{dt} = -\frac{1}{2} C_{Da}\rho|\vec{u}_{ra}|\vec{u}_{ra}A_2 a^2 + \rho\beta A_3 a^3 \frac{D\vec{u}_f}{Dt} - \rho g A_3 a^3 \quad (9)$$

CD: friction coefficient,: sediment velocity vector, : water velocity vector, : water velocity vector =σ/4, A3= σ/6 and d: Particle grain size, CM: Hypothetical mass coefficient (=0.5),: density of sediment, ρ: density of water, μf: static friction coefficient only when the particle is in the river bed. This term was determined according to Nakagawa's et al. For the simulation of successive saltation movement we followed Gotoh's method. Where is virtual mass given as 0.5, ρ is water density, is air bubble diameter, CDa: Friction coeffician of air bubble given as 2.6.

6. Results and discussions

In this section the authors only present results and discussions for the 25º slope angle case study. Particle routing movements for the 25º slope angle case can be visualized by four cases. The first case is initial, no liquid-phase flow case. Fig.6a shows the captured image for this case. Four different shapes were employed to represent the particle path line. In this case no small particle images were captured. This means, big particles move faster rather than small particles. The longest distance of movement for big particles (circle shape) is 14.09cm and the shortest (diamond shape) is 5.74cm. The average velocity for this case is 0.19cm/ms. Suwa (1988) claim that the cause of the convergence of large particles at the front of a debris flow is caused by their faster longitudinal velocities than the surrounding small particles, a vertical particle-segregation concept is adopted here to explain the convergence of large particles at the front. Takahashi (1980) verified this theory in previous flume experiments study. The velocity varies from zero at the bottom to a high value in upper layer, and the mean velocity is somewhere in between the bottom and surface values, if grain sorting arises in the following layer and coarser particles are transferred to the upper part, those particle would be transported faster than the mean propagating velocity of the debris flow front.

Small particle images can be seen starting with liquid-phase flow. A group of white lines concentrated near the bottom while the black lines are at the upper part. It shows that big particles move upward and in contrast for small particles. The average velocities of big particles are faster than the small ones. The velocity is 2cm/ms faster. Fig.6b shows particle tracing captured by HSVC for starting with liquid-phase flow. Same phenomenon happens for intermediate (2s) case. Big particles move upward and faster than small particles. The average velocity of the big particles is 4cm/ms faster than the small particles. From this captured image, we can understand the characteristics of particle movements between particles of different sizes.

(a)

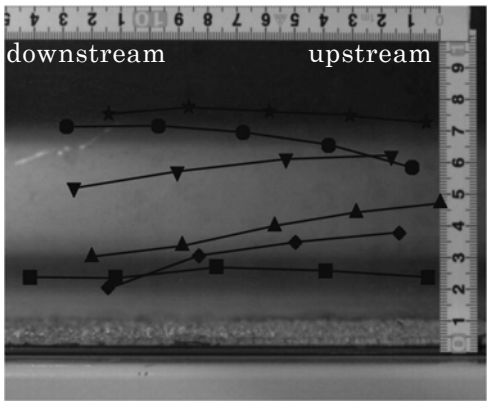

(b)

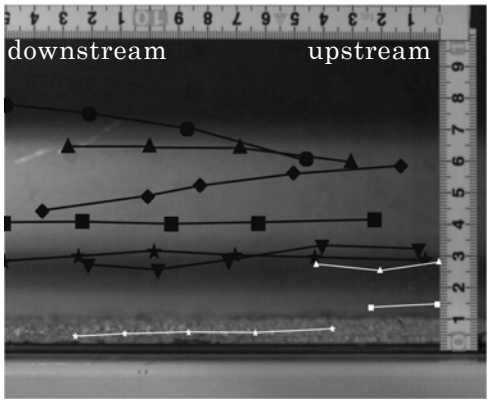

(c)

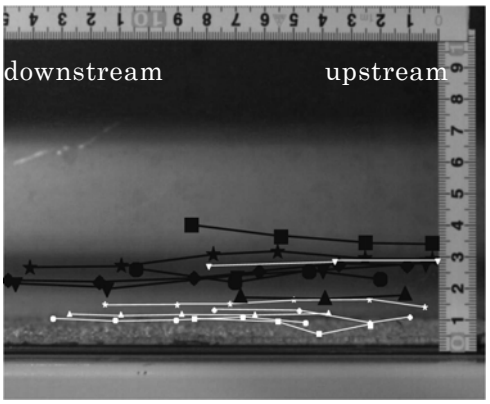

(d)

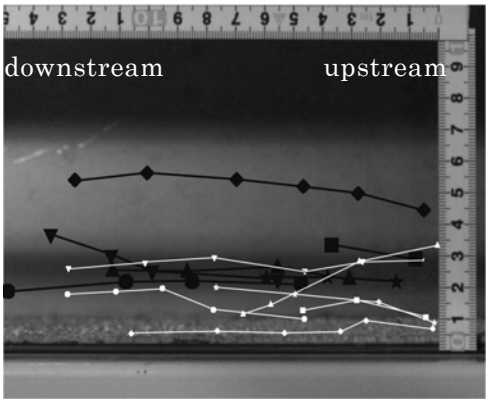

Fig. 6: Particle tracing captured by HSVC (a) initial, no liquid-phase flow (b) starting with liquid-phase flow (c) intermediate, 2s (d) last, 4s

For the last (4s) case, the average velocities of big and small particle are 0.15cm/ms and 0.13cm/ms respectively. The difference in velocity is 2cm/ms between the two particle sizes. In Fig.6d we can see that the longest travel distance for small particles is 12cm and the shortest travel distance is 1.82cm. As a result we can declare that similar phenomenons occur for big and small particle routing movements for each case of the 25º slope angle case. Further investigations could be done to further the debris flow particle routing mechanism.

Preliminary results of HD2DM had been made. By referred at the HD2DM results, tracing of 10mm and 2.5mm particles can be seen. Bigger particles flow at the upper part, while smaller particles attach near to the bottom. These phenomenons happen at the same as what we observed in the experimental study.

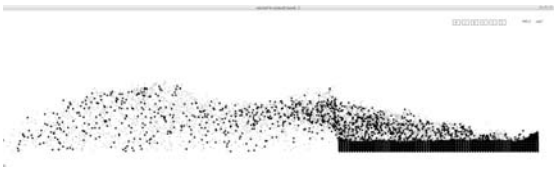

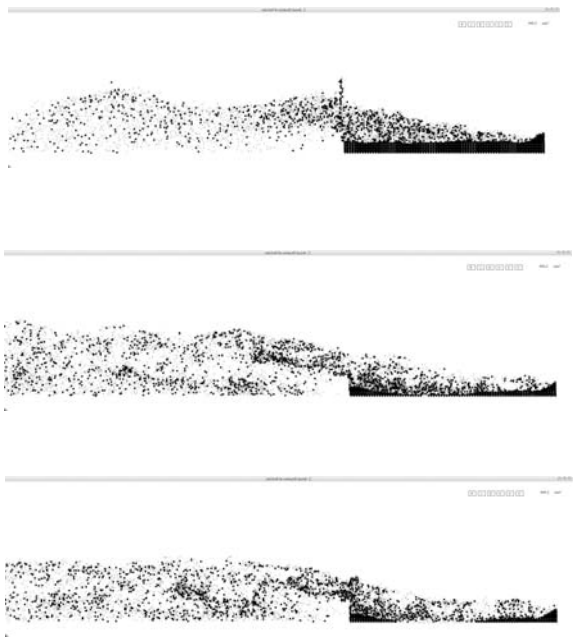

Fig. 7: Example results produced by HD2DM

The deposition formation observation had been done at three runs which were Run no. 1, Run no. 2 and Run no. 3. Fig. 8a to 8c shows three runs of material deposition formation of 25°. Fig.8a shows the highest deposition contour was 3cm and it is located at G6 and Row I-J and Column 6-8. The length of deposition trajectory is 130cm (Row N). Run no. 2 deposition pattern is showed in Fig.8b. The highest of deposition contour is located at G6, G8 and Row I-J and Column 6-8. The contour pattern and the trajectory length were nearly similar to Run no. 1 case. But the pattern of 2cm contour is slightly different. Fig.8c shows the deposition pattern for Run no. 3. The deposition trajectory for this case is the longest compared to two other cases. The length is 140cm (Row O). If we take a look at the deposition contour, the shape or pattern of the deposition looked similar in these three cases. But the number of 3cm contour is not the same. The average length for three cases is 133.33cm while the average width is 43.33cm. From the results we can observe if the trajectory length is shorter the width is thicker but if the trajectory length is longer the width length is thinner. For further understanding of deposition shape and pattern, sampling method should be conducted.

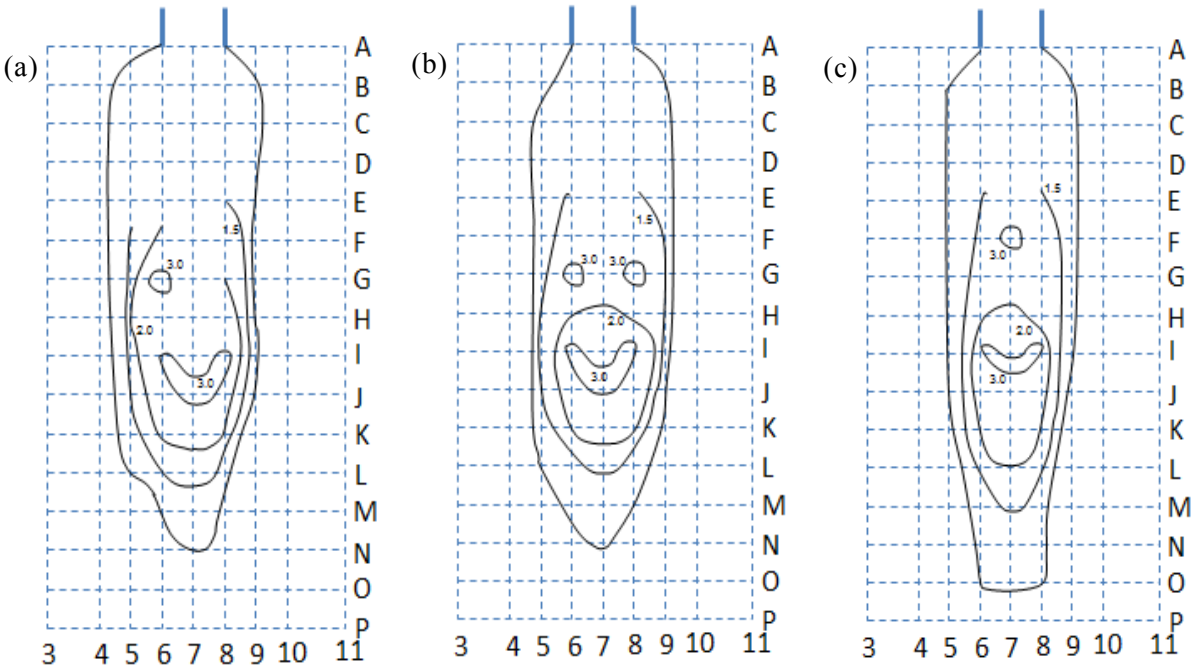

Fig. 8: Deposition pattern of 25º (a) Run no. 1 (b) Run no. 2 (c) Run no. 3

Table 3: The percentage of material at different nodes for (Run no. 1)

Node	Small (%)	Big (%)
C7	70	30
E7	76	24
F6	84	16
G5	57	43
G7	100	0
H6	71	29
I5	95	5
I7	86	14
J6	79	21
K7	88	12
L6	49	51
M7	0	100

Table 4: The percentage of materials at different nodes (Run no. 2)

Node	Small (%)	Big (%)
C7	61	39
D6	44	56
E7	59	41
F6	91	9
G7	98	2
H6	74	26
I7	56	44
J6	55	45
K7	25	75
L6	16	84
M7	2	98

Table 5: The percentage of materials at different nodes (Run no. 3)

Node	Small (%)	Big (%)
C7	71	29
D6	100	0
E7	70	30
F6	70	30
G7	64	36
H6	78	22
I7	84	16
J6	62	38
K7	51	49
L6	29	71
M7	32	68
N6	0	100
O7	0	100

The result of sampling method shows in Table 3 to Table 5. Table 3 shows the percentage of materials for Run no. 1. For the sampling reason, 12 nodes were selected in this case. The percentage of small particles was higher than big particles from nodes C7 to K7. In contrast, the percentage of big material was less. But at the head of deposition, percentage of big material is more than small material. Red box indicate higher percentage of big materials. The same characteristics were observed in Run no. 2 and 3. Big material conquered at the head part of the deposition. Many researchers had been reported

about this phenomenon (Takahashi, 1992; Major, 1997; Suwa et al., 1993).

7. Conclusions

The materials composition at deposition area clearly showed the characteristics of the particle segregation. This data can be used as an input data for computational numerical simulation. It was found that as soon as debris flow is produced on the well-graded sediment bed, larger particles move upwards while smaller particles remains in the bottom and the inverse grading in the debris flow becomes evident.

The following future works will be done for this research. The HD2DM using the soil erosion process qualitatively can be described as a well-performing model dealing with the process of particle motion. Analyses of the HSVC fully demonstrated the debris flow development mechanism. The following future works will be done: (1) some modification focusing on the particle movement mechanism (bed load motion), (2) developing a model for the deposition mechanism characteristics, and (3) Hydro Debris-3D Model (HD3DM).

Acknowledgements

This research was carried out with financial support from the Japanese Science and Technology Agency (JST) and also GCOE-HSE, Kyoto University. Also thanks to Mr. Fujiki Shigeo and Ms. Maya Ostric for their assistance in performing the experiments.

References

Arattano, M., and Grattoni, P. (2000): Using a fixed video camera to measure debris-flow surface velocity. In Debris-Flow Hazards Mitigation: Mechanics, Prediction, and Assessment, Proceedings of the 2nd International Conference. Edited by G.F. Wieczorek and N.D. Naeser. A.A. Balkema, Rotterdam. pp. 273–281.

Bagnold R.A. (1954): Experiments on a gravity-free dispersion of large solid spheres in a Newtonian fluid under shear, Proceedings of the Royal Society of London, Vol. 225A, pp. 49-63.

Ikeda, A., and Hara, Y. (2003): Flow properties of debris flows on the Kitamata Valley of the Name River, Japan. In Debris-Flow Hazards Mitigation: Mechanics, Prediction, and Assessment, Proceedings of the 3rd International Conference, Edited by D. Rickenmann and C.-L, Chen. Millpress, Rotterdam, pp. 851–862.

Inaba, H., Uddin, M.S., Itakura, Y., and Kasahara, M. (1997): Surface velocity vector field measurements of debris flow based on spatio temporal derivative space method, In Debris-Flow Hazards Mitigation: Mechanics, Prediction, and Assessment, Proceedings of the 1st International Conference, Edited by C.-L. Chen, American Society of Civil Engineers, New York, pp. 757–766.

Inaba, H., and Itakura, Y. (2003): Notes on the modeling of debris-flow surface images, In Debris-Flow Hazards Mitigation: Mechanics, Prediction, and Assessment, Proceedings of the 3rd International Conference. Edited by D. Rickenmann and C.-L. Chen, Millpress, Rotterdam. pp. 755–765

Innes, J. L. (1985): Magnitude-frequency relations of debris flows in northwest Europe Geogr. Ann. 61 A, pp. 23-32.

Iverson, R.M. (1997): The physics of the debris flows, American Geophysics Union, Vol. 97RG00426, pp. 245-296.

Jan, C. D., (1997): A study on the numerical modelling of debris flow, Debris Flow Hazard Miigation.: Mech., Pred. and Assessment, ASCE.

Johnson, A.M. (1984): Debris flowin slope instability, edited by D. Brunsden and D.B. Prior, John Wiley, New York, pp. 257-361.

Kano, M., Kobayashi, T. and Ishihara, T. (1985): Prediction of turbulent flow in two-dimensional channel with turbulent promoters, Mechanical Engineering Research, Vol. 50, pp. 449.

Lavigne, F., Tirel, A., Le Floch, D., and Veyrat-Charvillion, S. (2003): A real-time assessment of lahar dynamics and sediment load based on video-camera recording at Semeru volcano, Indonesia, In Debris-Flow Hazards Mitigation: Mechanics, Prediction, and Assessment, Proceedings of the 3rd International

Conference. Edited by D. Rickenmann and C.-L. Chen. Millpress, Rotterdam. pp. 871–882.
Lin, M.L., Jeng, F.S., (2000): Characteristics of hazards induced by extremely heavy rainfall in Central Taiwan—Typhoon Herb, Engineering Geology, Vol. 58, pp. 191–207.
Major, J.J., (1997): Depositional Processes in Large-Scale Debris–Flow Experiments, Journal of Geology, Vol. 105, pp. 345-366.
Martinez, J.M., Avila, G., Agudelo, A., Schuster, R.L., Casadevall, T.J..and Scott, K.M. (1995): Landslides and debris flows triggered by the 6 June 1994 Paez earthquake, southwestern Colombia. Landslide News 9, pp. 13-15.
Prochaska, A.B., Santi, P.M., and Higgins, J.D. (2008): Relationships between size and velocity for particles within debris flows, Canada Geotech. Journal, Vol. 45, pp. 1778-1783.
Smagolinsky, J. (1963): Monthly Weather Revision, Vol. 93, pp. 99.
Strunk, H., (1991): Frequency distribution of debris flows in the Alps since the 'Little Ice Age'. In: De Ploey, J., Haase, G., Leser, H. (Eds.), Geomorphology and Geoecology. V. Geomorphological Approaches in Applied Geography. Proc. 2nd Int. Conf. Geom., Frankfurt/Main, 1989 Zeitschrift für Geomorphologie Neue Folge Supplementband, Vol. 83, pp. 71–81.
Suwa, H. (1988): Focusing mechanism of large boulders to a debris flow front, Trans., Japanese Geomorphological Union, Kyoto, Japan, Vol. 9, No. 3, pp. 151-178.
Suwa, H., Okunishi, K. and Sakai, M (1993): Motion, debris size and scale of debris flow in a valley on Mount Yakedake, Japan, Proceeding of the Yokohama Symposium, IAHS Publication no. 217, pp. 239-248.
Takahashi, T. 1980: Debris Flow on Prismatic Open Channel, Journal Hidraulic Division, ASCE, Vol. 106, No. 3, pp. 381-396.
Takahashi, (1981): Estimation of potential debris flows and their hazardous zones; soft countermeasures for a disaster, Journal of Natural Disaster Science, Vol. 3, pp. 57-89.
Takahashi, T., Nakagawa, H., Harada, T., and Yamashiki Y. (1992): Routing debris flows with particle segregation, Journal of Hydraulic Engineering, Vol. 118, pp. 1490-1570.
Takahashi, T. (2009): A Review of Japanese Debris Flow Research, International Journal of Erosion Control Engineering, ASCE, Vol. 2, No. 1, pp. 1-14.
Tecca, P.R., Deganutti, A.M., Genevois, R., and Galgaro, A. (2003): Velocity distributions in a coarse debris flow, In Debris-Flow Hazards Mitigation: Mechanics, Prediction, and Assessment, Proceedings of the 3rd International Conference, Edited by D. Rickenmann and C.-L. Chen. Millpress, Rotterdam. pp. 905–916.
Van Steijn, H., Coutard, J.-P., (1989): Laboratory experiments with small debris flows: physical properties related to sedimentary characteristics, Earth Surface Processes and Landforms, Vol. 14, pp. 587-596.
Villi, and Dal Pra, A. (2002): Debris flow in the upper Isarco valley, Italy, 14 August 1998, Bulletin of Engineering Geology and the Environment, Vol. 61, pp. 49-57.
Yamashiki Y., Takahashi T., De Souza P. A., and Tamada K. (1997): Numerical Simulation of Large Eddy Structure in Hydraulic Jump, Proceedings of the 27th Congress of the International Association for Hydraulic Research, ASCE, Proceedings of Theme D, pp. 228-233.
Zhang, S., and Chen, J. 2003. Measurement of debris-flow surface characteristics through close-range photogrammetry, In Debris-Flow Hazards Mitigation: Mechanics, Prediction, and Assessment, Proceedings of the 3rd International Conference. Edited by D. Rickenmann and C.-L. Chen. Millpress, Rotterdam, pp. 775–784.

石灰岩の土石流のメカニズムとその流動特性に関する研究

Remy Rozainy M. A. Z *・山敷庸亮・松本拓・高橋 保・寶馨

*京都大学工学研究科都市環境工学専攻

要　旨

本研究では急斜面の土石流の実験水路を用いた。土石流における大きいな被害と多い死傷者を引き起こすのことがあるので，大きい粒子運動の特性を実験するのは，重要である。 この研究は2つの異なった粒径（10mmと2.5mm）の土石流開発のメカニズムを示している。この研究は1つの傾斜度（25°）を使っていた。一定の流量(3.01/s)が7秒の持続時間に供給された。粒子運動は，目視により個々の粒子粒の運動特性を得るのに，高速ビデオカメラ(HSVC)を使用することによって分析された。水文土石流－2D モデル(HD2DM)は，ラグランジアンの沈殿物の粒子の追跡の数字の実験に基づいて開発された。それぞれの粒子運動をたどるHSVC結果は，HD2DMシミュレーションの結果と比較した。

キーワード:土石流，高速ビデオカメラ（HSVC)，ラグランジュ，水文土石流－2D モデル(HD2DM)